BMB Reports - Manuscript Submission

Manuscript Draft

Manuscript Number: BMB-21-051

Title: Perilipin 5 is a novel target of nuclear receptor LRH-1 to regulate hepatic triglycerides metabolism

Article Type: Article

Keywords: LRH-1; PLIN5; Liver; Hepatic triglycerides; Fasting

Corresponding Author: Seung-Soon Im

Authors: Rubee Pantha[1], Jae-Ho Lee[1], Jae-Hoon Bae[1], Eun Hee Koh[2], Minsang Shin[3], Dae-Kyu Song[1], Seung-Soon Im[1,*]

Institution: [1]Physiology, Keimyung University School of Medicine, Daegu 42601, Republic of Korea,
[2]Internal Medicine, University of Ulsan College of Medicine, Seoul, 05505 Republic of Korea,
[3]Microbiology, School of Medicine, Kyungpook National University, 680 Gukchaebosang-Ro, Jung-gu, Daegu, 41944, South Korea,

Manuscript Type: Article

Title: Perilipin 5 is a novel target of nuclear receptor LRH-1 to regulate hepatic triglycerides metabolism

Author's name: Rubee Pantha[1], Jae-Ho Lee[1], Jae-Hoon Bae[1], Eun Hee Koh[2], Minsang Shin[3], Dae-Kyu Song[1], Seung-Soon Im[1*]

Affiliation: [1]Department of Physiology, Keimyung University School of Medicine, 1095 Dalgubeol-daero, Dalseo-gu, Daegu 42601, Republic of Korea

[2]Department of Internal Medicine, Asan Institute for Life Science, University of Ulsan College of Medicine, 88, Olympic-ro 43-gil, Songpa-gu, Seoul, 05505, Republic of Korea

[3]Department of Microbiology, School of Medicine, Kyungpook National University, 680 Gukchaebosang-Ro, Jung-gu, Daegu, 41944, South Korea

Running Title: LRH-1 resolves hepatic lipid accumulation via PLIN5.

Keywords: Liver receptor homolog-1, Perilipin 5, Triglycerides, Fasting, Lipid droplet.

Corresponding Author's Information: Prof. Seung-Soon Im, Tel: +82-53-258-7423; Fax: +82-53-258-7412; email: ssim73@kmu.ac.kr

ABSTRACT

Liver receptor homolog-1 (LRH-1) has emerged as a regulator of hepatic glucose, bile acid, and mitochondrial metabolism. However, the functional mechanism underlying the effect of LRH-1 on lipid mobilization has not been addressed. This study investigated the regulatory function of LRH-1 in lipid metabolism in maintaining a normal liver physiological state during fasting. The Lrh-$1^{f/f}$ and LRH-1 liver-specific knockout (Lrh-1^{LKO}) mice were either fed or fasted for 24 h, and the liver and serum were isolated. The livers were used for qPCR, western blot, and histological analysis. Primary hepatocytes were isolated for immunocytochemistry assessments of lipids. During fasting, the Lrh-1^{LKO} mice showed increased accumulation of triglycerides in the liver compared to that in Lrh-$1^{f/f}$ mice. Interestingly, in the Lrh-1^{LKO} liver, decreases in perilipin 5 (PLIN5) expression and genes involved in β-oxidation were observed. In addition, the LRH-1 agonist dialauroylphosphatidylcholine also enhanced PLIN5 expression in human cultured HepG2 cells. To identify new target genes of LRH-1, these findings directed us to analyze the *PLIN5* promoter sequence, which revealed −1620/−1614 to be a putative binding site for LRH-1. This was confirmed by promoter activity and chromatin immuno-precipitation assays. Additionally, fasted Lrh-$1^{f/f}$ primary hepatocytes showed increased co-localization of PLIN5 in lipid droplets (LDs) compared to that in fasted Lrh-1^{LKO} primary hepatocytes. Overall, these findings suggest that PLIN5 might be a novel target of LRH-1 to mobilize LDs, protect the liver from lipid overload, and manage the cellular needs during fasting.

INTRODUCTION

Liver receptor homolog-1 (LRH-1/NR5A2) is a representative of the nuclear receptor 5A subfamily of orphan nuclear receptors, mainly expressed in the liver, pancreas, ovary, and intestine (1). It is the principal regulator of glucose, bile acid, and cholesterol metabolism with varied biological roles extending from regulation of the cell cycle to the maintenance of steroid homeostasis (2, 3). In the pancreas, LRH-1 with pancreas transcription factor stimulates the expression of genes encoding pancreatic digestive enzymes and secretory proteins (4). Moreover, LRH-1 regulates the maturation of ovarian follicles and ovulation in the ovary (5) and is responsible for mitochondrial function by regulating cytochrome p450, family 11, subfamily a, polypeptide 1 and cytochrome p450, family 11, subfamily b, polypeptide 1 in the intestinal epithelium (6). In the liver, LRH-1 is involved in mitochondrial biogenesis and β-oxidation through the regulation of peroxisome proliferator-activated receptor gamma coactivator 1-alpha gene expression (PGC-1α) (7). It is also involved in maintaining the pool of arachidonoyl phospholipids, which are important for normal lipid homeostasis in the liver (8). In addition, LRH-1 liver-specific knockout ($Lrh\text{-}1^{LKO}$) mice show endoplasmic reticulum stress-induced fatty liver, indicating that LRH-1 plays a major role in triglyceride (TG) accumulation in the liver (9).

Excess TGs in the liver are mainly reserved within lipid droplets (LDs) (10). LDs are used to balance lipid storage and utilization and are strongly regulated in a cell type-specific manner (11). As LDs modulate low intracellular free fatty acid levels, they play a crucial role in protecting the liver from lipotoxicity caused by excess fatty acids in nutritional stress conditions (10, 12). In addition, the mobilization of LDs reflects the metabolic state of cells and also indicates changes in the LD-related proteins that contribute to the regulation of lipid metabolism and lipid homeostasis (13).

The perilipin (PLIN) protein family, which attaches to LDs, is a representative group of LD-associated proteins that utilizes the stored lipids of LDs via lipolysis (10, 11). It is composed of five members, named PLIN1–5 and is classified based on stability in a free state. PLIN1 and PLIN2 rapidly degrade in a free state; however, they exist when bound to LDs. The remaining proteins from the family, PLIN3, PLIN4, and PLIN5, are found either free in the cytosol or lining the LDs (14). PLIN1 is found in white and brown adipose tissue (WAT and BAT), whereas PLIN2 and PLIN3 are distributed in many cell types, and PLIN2 is especially observed in hepatocytes. PLIN4 is expressed in cardiomyocytes, adipocytes, and myocytes, and PLIN5 is usually confined within tissues or cells with high oxidative capacity, namely the liver, heart, BAT, and muscle (11, 14, 15).

Among the PLIN family, PLIN5 has emerged as indispensable for adjusting lipid abundance. It is highly active upon fatty acid treatment in cultured cells, with a high-fat diet, and upon prolonged fasting (10). Prolonged fasting is also known to increase TGs accumulation in the liver (16, 17) due to increased adipose tissue lipolysis (18). Therefore, PLIN5 is also regarded as the regulator of TGs metabolism (19). The overexpression of PLIN5 in cells enhances the expression of genes encoding proteins involved in aerobic catabolism and promotes both TGs storage and fatty acid oxidation. Thus, PLIN5 rapidly mobilizes energy by sensing the nutrient demand (20).

The nuclear receptor LRH-1 is activated during nutritional stress and is involved in protecting the liver from lipid overload by increasing the β-oxidation. Even though LRH-1 regulates mitochondrial biogenesis and lipid metabolism, its regulatory mechanism and function under fasting conditions has not been completely addressed. Therefore, in this study, the regulatory function of LRH-1 was investigated during fasting state by utilizing Lrh-1$^{f/f}$ and Lrh-1^{LKO} mice to verify the function of LRH-1 in cellular energy demands and lipid

overloading state.

RESULTS

LRH-1 mitigates hepatic lipid overload by inducing the expression of PLIN5 and fatty acid oxidation-related genes

To understand the function of LRH-1 in regulating TGs during fasting, Lrh-1$^{f/f}$ and Lrh-1^{LKO} mice were either fed or starved for 24 h, and the liver (Fig. 1A) and serum were isolated to examine hepatic and serum TGs levels. Initially, serum β-hydroxybutyrate levels was measured in both Lrh-1$^{f/f}$ and Lrh-1^{LKO} mice to confirm the fasting condition. As expected, the fasting condition has increased serum β-hydroxybutyrate levels but did not show significant differences between the genotypes (Supplementary Fig. 2A). The livers from Lrh-1^{LKO} mice starved for 24 h displayed higher accumulation of lipids compared to that in livers of starved Lrh-1$^{f/f}$ mice in Oil red-O staining (Fig. 1B & 1C), implying the necessity for further analysis of lipid levels in the liver and serum. Interestingly, fasted Lrh-1^{LKO} mice exhibited remarkably escalated hepatic TGs levels compared to those in fasted Lrh-1$^{f/f}$ mice. However, there was no significant difference between the fed mice of either genotype (Fig. 1D). In contrast, hepatic cholesterol was not altered between the genotypes in either fed or starved conditions (Fig. 1E). Surprisingly, Lrh-1^{LKO} mice either fed or starved showed a notable decrease in serum TGs levels compared to those in Lrh-1$^{f/f}$ mice (Fig. 1F). However, serum cholesterol and non-esterified fatty acids (NEFA) levels were not altered significantly (Fig. 1G & 1H). These findings suggest that the loss of LRH-1 results in a buildup of lipids in the liver, indicating that LRH-1 might be a key regulator in balancing the hepatic lipid content.

To discover new potent target genes of LRH-1 involved in lipid metabolism, the mRNA and protein expression of various genes was examined in liver samples. The expression levels of

Lrh-1 (Fig. 1I) and its target gene (Fig. 1J) were highly reduced in Lrh-1^{LKO} livers which confirmed Lrh-1^{LKO} mice.

In the liver, PLIN2 and PLIN5 are highly expressed (21) therefore, mRNA expression was measured. However, *Plin2* did not display significant difference between the genotypes in either fed or fasted conditions (Fig. 1K). In the liver, PLIN5 is known to regulate lipid metabolism (10) by promoting or inhibiting the hydrolysis of LDs (22). Next, the mRNA and protein expression of PLIN5 was measured. Interestingly, as *Lrh-1* expression was augmented, the *Plin5* level also increased in the livers of Lrh-1$^{f/f}$ fasted mice. However, the expression of *Plin5* was diminished markedly in the livers of either fed or starved Lrh-1^{LKO} mice (Fig. 1L).

Additionally, TGs and β-oxidation are strongly interconnected with lipid metabolism. To understand the different liver phenotypes in Lrh-1$^{f/f}$ and Lrh-1^{LKO} mice, the expression of genes involved in fatty acid β-oxidation was measured. Carnitine palmitoyltransferase-1 alpha (*Cpt-1α*), a regulator of fatty acid β-oxidation (23) and fibroblast growth factor 21 (*Fgf21*), an oxidation enhancer and lipogenesis inhibitor (24) were expressed at remarkably lower levels in the livers of either fed or starved Lrh-1^{LKO} mice. Nevertheless, expression was highly escalated in livers of Lrh-1$^{f/f}$ fasted mice (Fig. 1M & 1N). Similarly, peroxisome proliferator-activated receptor alpha (*Pparα*), a transcription factor that regulates *Cpt-1α* and *Fgf21*, significantly increased gene expression levels in Lrh-1$^{f/f}$ fast mice. However, gene expression levels were significantly decreased in both fed and fasted Lrh-1^{LKO} mice (Fig. 1O). Gene expression levels of *Pgc-1α* was increased during fasting but did not show significant differences between the genotypes (Fig. 1P). In addition, dialauroylphosphatidylcholine (DLPC), an LRH-1 agonist increased fatty acid oxidation-related genes in PLIN5 knockdown human cultured HepG2 cells (Supplementary Fig. 4). Moreover, protein levels of LRH-1, PLIN5, CPT-1α, and PGC-1α were measured in the liver samples (Fig. 1Q). Protein levels of

LRH-1 and PLIN5 were remarkably decreased in either fed or fasted Lrh-1^{LKO} mice. Also, protein levels of CPT-1α decreased in Lrh-1^{LKO} mice. These findings suggest that PLIN5 is a putative target of LRH-1, and that the loss of LRH-1 reduces the expression of β-oxidation-related genes.

LRH-1 agonist amplifies PLIN5 gene expression due to putative LRH-1 responsive elements (LRE) in PLIN5 promoter region

To determine whether PLIN5 is regulated by an LRH-1 agonist, human cultured HepG2 cells were treated with 100 μM DLPC for 24 h and the gene expression and protein levels of PLIN5 were measured. In the presence of DLPC, *PLIN5* mRNA expression (Fig. 2A) and protein levels (Fig. 2B & 2C) increased significantly. Although, DLPC treatment did not alter LRH-1 protein levels (Fig. 2C), the mRNA expression was increased (Fig. 2A). These observations indicate that PLIN5 could be regulated by an exogenous agonist of LRH-1, implying that LRH-1 guides PLIN5.

To discover potent LRH-1-regulated genes, putative LRE in the *PLIN5* promoter sequence were analyzed by Chromatin immunoprecipitation sequencing (ChIP-Seq) analysis using a published mouse ChIP-Seq data set for LRH-1 (25). As expected, the ChIP-Seq analysis of *PLIN5* resulted in the identification of LRE peaks in the promoter region (Fig. 2D). Furthermore, *PLIN5* proximal promoter sequences were mapped utilizing the UCSC genome browser to identify the putative LRE. The *PLIN5* promoter region was found to have four putative LRE with direct orientations (−112/−106, −719/−713, −976/−970, and −1620/−1614 from the transcription starting site; Supplementary Fig. 1A).

LRH-1 stimulates *PLIN5* promoter activity

To confirm whether LRH-1 controls *PLIN5* at a transcriptional level by binding its promoter, the *PLIN5* promoter region was cloned upstream of the luciferase expression reporter gene (Fig.

3A). The *PLIN5* promoter construct was co-transfected with or without the LRH-1 expression plasmid and cells were treated with 100 μM DLPC. The *PLIN5* promoter activity increased significantly in the presence of the LRH-1 expression vector and DLPC (Fig. 3B). In addition, to distinguish the main LRE among the four putative sites in the *PLIN5* promoter, each putative LRE was deleted from the construct. The deletion at the putative site −1620/−1614 diminished luciferase activity in response to LRH-1 in comparison to that with the other sites (Fig. 3C).

This finding shows that −1620/−1614 in the *PLIN5* promoter region was the conserved site for LRH-1 binding and its removal in the construct diminished the response to LRH-1. Furthermore, binding of the LRH-1 at the −1620/−1614 site was verified by a ChIP assay performed on liver samples from 24 h-fasted and fed Lrh-1$^{f/f}$ and Lrh-1^{LKO} mice. When the sample was treated with the LRH-1 antibody, enrichment of the LRE −1620/−1614 was markedly elevated in livers of fasted Lrh-1$^{f/f}$ mice compared to that in fed Lrh-1$^{f/f}$ mice. Moreover, there were significant differences between the genotypes for either fed or starved mice (Fig. 3D). In addition, electrophoretic mobility shift assay (EMSA) was also performed to confirm the binding of LRH-1 at the -1620/-1614 region of the PLIN5 promoter sequence. The radiolabeled DNA probe corresponding to -1620/-1614 region which includes LRE were incubated with LRH-1 overexpressed nuclear extract proteins. Thus, DNA-LRH-1 complex resulted in supershift while unlabeled cold DNA reduced the supershift (Supplementary Fig. 3). Moreover, Lrh-1^{LKO} mice decreased the enrichment of LRH-1 on PLIN5 gene promoter (Supplementary Fig. 1B). These results suggested that the −1620/−1614 site in the *PLIN5* promoter region is responsible for the transcriptional regulation by LRH-1.

LRH-1 controls PLIN5 to regulate LDs in mouse hepatocytes during nutritional stress

To evaluate the regulation of LDs via LRH-1, primary hepatocytes were isolated from Lrh-1$^{f/f}$ and Lrh-1^{LKO} mice to perform BODIPY staining. Primary hepatocytes were grown either in

complete (fed) or fasting media to understand the regulatory mechanism of LRH-1 during fasting in the liver. In the fasting media, PLIN5 surrounding the LDs was more abundant in the Lrh-$1^{f/f}$ hepatocytes than in the Lrh-1^{LKO} hepatocytes. Moreover, fasting condition increased LDs number in Lrh-1^{LKO} hepatocytes relative to that in Lrh-$1^{f/f}$ hepatocytes. Nevertheless, the sizes of the LDs in Lrh-$1^{f/f}$ hepatocytes were found to be distinct and increased compared to that in Lrh-1^{LKO} hepatocytes (Fig. 4A & 4C). Additionally, in fasting condition, the co-localization of PLIN5 in LDs was increased in Lrh-$1^{f/f}$ hepatocytes compared to that in complete media (Fig. 4B).

Next, to verify alterations in the lipid quantity in the liver and serum, the mRNA expression of microsomal triglyceride transfer protein (*Mttp*), a key gene responsible for the assembly and release of lipoproteins, was measured. The Lrh-1^{LKO} mice either fed or starved showed remarkably decreased *Mttp* mRNA expression compared to that in Lrh-$1^{f/f}$ mice (Fig. 4D). Furthermore, expression of the apolipoprotein B (*ApoB*) gene, a principal component present in very low-density lipoproteins (VLDLs) was measured. However, there was no significant differences between the genotypes (Fig. 4D). In addition, PLIN5 dependent hepatic TGs accumulation during fasting in Lrh-1^{LKO} mice was confirmed by overexpressing PLIN5 in the Lrh-1^{LKO} mice (Supplementary Fig. 2B). The PLIN5 overexpressed Lrh-1^{LKO} mice significantly decreased hepatic TGs accumulation compared to that of the control Lrh-1^{LKO} mice (Fig. 4E). Taken together, PLIN5 recovers the fasting-induced TGs accumulation in the Lrh-1^{LKO} mice, and the loss of LRH-1 decreases PLIN5 co-localization in the LDs. Moreover, LRH-1 deficiency increases TGs in the liver by decreasing TGs secretion, leading to a surplus in the LDs.

DISCUSSION

Hepatic LRH-1 is a transcriptional regulator of glucose metabolism and bile acid homeostasis

(26). This study discovered PLIN5 as a direct target of LRH-1 and explored the function of LRH-1 in the liver during fasting. In this study, fasting increased the accumulation of liver TGs more readily in the Lrh-1^{LKO} livers compared to that in Lrh-1$^{f/f}$ livers. The elevation of hepatic TGs in the liver might be due to a decrease in β-oxidation. As expected, livers of Lrh-1^{LKO} mice either fed or starved showed the markedly diminished expression of key genes responsible for β-oxidation, as well as their enhancer gene, indicating the possible accumulation of lipids in the liver. Recent studies on Lrh-1^{LKO} mice revealed that LRH-1 promotes β-oxidation and mitochondrial biogenesis (7). Incidentally, this result coincides with the previous findings in PLIN5^{LKO} mice, demonstrating elevated hepatic TGs levels and a reduction in fatty acid oxidation in the liver (10). However, these findings were in contrast with the reported research performed by Wang et al (27). They reported decreased TGs in the liver and increased β-oxidation in the whole body PLIN5-KO mice. Together, this suggests close phenotypic similarity between LRH-1 and PLIN5 due to the transcriptional regulation of PLIN5 by LRH-1.

Interestingly, starved Lrh-1^{LKO} mice exhibited a decrease in serum TGs levels compared to that in Lrh-1$^{f/f}$ mice. Altered liver and serum TGs levels between the genotypes were also observed, which might be due to a decrease in TGs secretion from the liver (28). Therefore, the genes involved in VLDL secretion from the liver were measured. The gene expression of *Mttp*, a key player in VLDL secretion was markedly decreased in the livers of Lrh-1^{LKO} mice; however, *ApoB* was unaltered. Furthermore, a decrease in TGs secretion was reported in PLIN5^{LKO} mice (10). Collectively, these data suggest that MTTP might be responsible for decreasing serum TGs in the livers of Lrh-1^{LKO} mice.

Transcription factors often bind and sense lipid molecules (29). LRH-1 binds to the −1620/−1614 binding sequence in the *PLIN5* promoter region for its transcriptional regulation,

which was confirmed by promoter activity, ChIP assays and EMSA. In addition, DLPC, as an agonist of LRH-1, which has a previously established role in the synthesis of bile acids and reduction of hepatic TGs (30), increases the mRNA expression of *PLIN5*. Therefore, these findings indicate that LRH-1 regulates PLIN5 at the transcriptional level.

PLIN5 balances fatty acid requirements to meet cellular needs, protecting mitochondria during extreme fatty acid flux with low-energy demands and encouraging fatty acid mobilization and oxidation with high-energy demands (31). Based on BODIPY staining, starved Lrh-1$^{f/f}$ hepatocytes demonstrated the utilization of LDs, whereas lipids were accumulated in the fasted Lrh-1^{LKO} hepatocytes. Furthermore, PLIN5 and BODIPY staining clearly resulted in more intense red and green fluorescence, respectively, implying the co-localization of PLIN5 in LDs during starvation in Lrh-1$^{f/f}$ hepatocytes. This indicates that the loss of LRH-1 decreases PLIN5 co-localization in LDs and increases the lipid content. Surprisingly, in the starved Lrh-1$^{f/f}$ hepatocytes, the size of the LDs was increased and distinct compared to that in starved Lrh-1^{LKO} hepatocytes. However, the quantity of lipids was increased in the fasted Lrh-1^{LKO} hepatocytes. A previous study reported a decrease in the amount and size of LDs in the whole body PLIN5-KO mice (27). Nevertheless, in this study, the number of LDs increased in the Lrh-1^{LKO} mice. PLIN5 regulates both the storage and usage of TGs and is regarded as metabolically protective (32). In fasted Lrh-1$^{f/f}$ hepatocytes, LRH-1 regulates PLIN5 to protect the liver by increasing the influx of TGs within the LDs. As a result, this increases the size of LDs. In addition, it promotes fatty acid oxidation to meet cellular energy demands during starvation, resulting in fewer LDs. In contrast, the lack of LRH-1 in the Lrh-1^{LKO} mice attenuated PLIN5 expression, resulting in small-sized LDs and increasing their numbers (Fig. 4F). This might be the mechanism underlying the changes in the size and quantity of LDs, respectively. Furthermore, the overexpression of PLIN5 decreased the fasting-

induced TGs accumulation in the Lrh-1^{LKO} liver, which confirmed the significant role of PLIN5 expression in regulating TGs metabolism. Overall, these observations indicate that LRH-1 regulates PLIN5 to mobilize LDs and balances hepatic lipid contents.

In summary, this study uncovered the function of LRH-1 in the liver during fasting and presents a novel target of LRH-1 in the liver. Results further suggest the necessity of LRH-1 in lipid management to protect the liver from lipid accumulation. In the liver, LRH-1 regulates PLIN5 to mobilize lipids and maintains this balance during fasting conditions. Additionally, LRH-1 regulates PLIN5 to equilibrate the cellular needs and storage of lipids, thus protecting the liver from metabolic diseases associated with a fatty liver. Although LRH-1 is involved in managing the lipid content in the liver, further studies are required to assess the possible targeting of this molecule for the treatment of nonalcoholic steatohepatitis. Thus, this study might be a platform to elucidate the mechanism underlying the treatment of nonalcoholic steatohepatitis and could be beneficial for the protection of the liver.

MATERIALS AND METHODS

The detailed methods are described in the “Supplementary Information”.

ACKNOWLEDGMENTS

This study was supported by grants of the Korea Research Foundation, an NRF grant funded by the Korea Government (MSIP) (2019R1A2C2085302, NRF-2021R1A4A1029238) and KMPC (2015R1D1A1AO1057610).

CONFLICTS OF INTEREST

The authors declare no conflict of interest.

FIGURE LEGENDS

Fig. 1. Increased hepatic lipid contents in fasted Lrh-1^{LKO} mice via decreased β-oxidation genes. All experiments were performed in 24 h-fasted or fed Lrh-1$^{f/f}$ and Lrh-1^{LKO} mice (A) Dissection image of 24 h-fasted or fed Lrh-1$^{f/f}$ and Lrh-1^{LKO} mice along with their isolated livers. (B) Oil red-O staining of liver tissue (scale bar = 30 μm). (C) Quantification of staining in % area shown in B. (D) Hepatic triglycerides levels. (E) Hepatic cholesterol levels. (F) Serum triglycerides levels. (G) Serum cholesterol levels. (H) Serum NEFA levels. (n = 4/group). (I, J) mRNA expression level of *Lrh-1* and its target gene. (K, L) mRNA expression levels of *Plin2* and *Plin5* respectively. (M, N) mRNA expression of *Cpt-1α* and *Fgf21* respectively. (O, P) mRNA expression of *Pparα* and *Pgc-1α,* respectively. (n = 5/group). (Q) Western blot for protein analysis. GAPDH was used as a loading control. $^{\#}p < 0.05$, $^{\#\#}p < 0.01$, $^{\#\#\#}p < 0.001$, Lrh-1$^{f/f}$ vs. Lrh-1^{LKO}, $^{***}p < 0.001$, Lrh-1$^{f/f}$ fed vs. Lrh-1$^{f/f}$ fast.

Fig. 2. LRH-1 agonist elevates PLIN5 gene expression. (A) mRNA expression of *LRH-1* and *PLIN5* gene after DLPC treatment. (B) Western blot for protein analysis of PLIN5 and LRH-1 after DLPC treatment. (C) LRH-1 and PLIN5 protein fold change relative to β-actin which was used as a loading control. These experiments were performed in triplicate. $^{\#\#}p < 0.01$, $^{\#\#\#}p < 0.001$, Mock vs. DLPC. (D) LRH-1 response elements on the mouse liver chromosome were obtained from the LRH-1. ChIP-Seq data and identified peaks that mapped to the mouse PLIN5 promoter using the UCSC Genome Browser. ChIP-Seq, chromatin immunoprecipitation sequencing.

Fig. 3. LRE in the PLIN5 promoter is responsive to LRH-1. (A) Representation of putative LRE in PLIN5 promoter region. (B) HEK-293T cells were transfected with pmPLIN5 containing the PLIN5 promoter upstream of the luciferase reporter gene along with a pcDNA

or LRH-1 expression vector. (C) LRH-1 deletion mutants from the PLIN5 promoter region co-transfected with pcDNA or LRH-1 expression vector. The deleted sequences were shown in boxes. These experiments were performed in triplicate. $^{\#}p < 0.05$, pcDNA vs pcLRH-1, $^{*}p < 0.05$ WT pcLRH-1 vs M1pcLRH-1. (D) ChIP assay measured in 24 h-fasted or fed Lrh-$1^{f/f}$ and Lrh-1^{LKO} livers. (n = 3/group). $^{\#\#\#}p < 0.001$, Lrh-$1^{f/f}$ fast vs. Lrh-1^{LKO} fast, $^{**}p < 0.01$, Lrh-$1^{f/f}$ fed vs. Lrh-$1^{f/f}$ fast.

Fig. 4. LRH-1 mobilizes hepatic LDs via PLIN5. (A) BODIPY staining in primary hepatocytes grown in complete (fed) or fasting media followed by overnight incubation of PLIN5 antibody. (B) Co-localization of PLIN5 in LDs shown in A. (n = 3/treatment group) (C) Quantification data for the size of LDs shown in (A). (D) mRNA expression of genes related to VLDL secretion measured in 24 h-fasted or fed Lrh-$1^{f/f}$ and Lrh-1^{LKO} livers. (n = 5/group). (E) Hepatic triglycerides levels by PLIN5 overexpression in Lrh-$1^{f/f}$ and Lrh-1^{LKO} mice. (n = 4/group). $^{\#\#\#}p < 0.001$, $^{\#}p < 0.05$, Lrh-$1^{f/f}$ vs Lrh-1^{LKO}, $^{**}p < 0.01$, $^{*}p < 0.05$, Lrh-$1^{f/f}$ fed vs. Lrh-$1^{f/f}$ fast, $^{\S\S}p < 0.01$, Lrh-1^{LKO} pcDNA vs Lrh-1^{LKO} pcPLIN5. (D) Scheme illustrating the role of LRH-1 in liver during fasting.

REFERENCES

1. Fayard E, Auwerx J and Schoonjans K (2004) LRH-1: an orphan nuclear receptor involved in development, metabolism and steroidogenesis. Trends Cell Biol 14, 250-260
2. Stein S, Lemos V, Xu P et al (2017) Impaired SUMOylation of nuclear receptor LRH-1 promotes nonalcoholic fatty liver disease. J Clin Invest 127, 583-592
3. Schwaderer J, Phan TS, Glockner A et al (2020) Pharmacological LRH-1/Nr5a2 inhibition limits pro-inflammatory cytokine production in macrophages and associated experimental hepatitis. Cell Death Dis 11, 154
4. Holmstrom SR, Deering T, Swift GH et al (2011) LRH-1 and PTF1-L coregulate an exocrine pancreas-specific transcriptional network for digestive function. Genes Dev 25, 1674-1679
5. Duggavathi R, Volle DH, Mataki C et al (2008) Liver receptor homolog 1 is essential for ovulation. Genes Dev 22, 1871-1876
6. Mueller M, Cima I, Noti M et al (2006) The nuclear receptor LRH-1 critically regulates extra-adrenal glucocorticoid synthesis in the intestine. J Exp Med 203, 2057-2062
7. Choi S, Dong B, Lin CJ et al (2020) Methyl-sensing nuclear receptor liver receptor homolog-1 regulates mitochondrial function in mouse hepatocytes. Hepatology 71, 1055-1069
8. Miranda DA, Krause WC, Cazenave-Gassiot A et al (2018) LRH-1 regulates hepatic lipid homeostasis and maintains arachidonoyl phospholipid pools critical for phospholipid diversity. JCI Insight 3, e96151
9. Mamrosh JL, Lee JM, Wagner M et al (2014) Nuclear receptor LRH-1/NR5A2 is required and targetable for liver endoplasmic reticulum stress resolution. Elife 3,

e01694

10. Keenan SN, Meex RC, Lo JCY et al (2019) Perilipin 5 deletion in hepatocytes remodels lipid metabolism and causes hepatic insulin resistance in mice. Diabetes 68, 543-555
11. Kimmel AR and Sztalryd C (2014) Perilipin 5, a lipid droplet protein adapted to mitochondrial energy utilization. Curr Opin Lipidol 25, 110-117
12. Khor VK, Shen WJ and Kraemer FB (2013) Lipid droplet metabolism. Curr Opin Clin Nutr Metab Care 16, 632-637
13. Pol A, Gross SP and Parton RG (2014) Review: biogenesis of the multifunctional lipid droplet: lipids, proteins, and sites. J Cell Biol 204, 635-646
14. Langhi C, Marquart TJ, Allen RM and Baldan A (2014) Perilipin-5 is regulated by statins and controls triglyceride contents in the hepatocyte. J Hepatol 61, 358-365
15. Tan Y, Jin Y, Wang Q, Huang J, Wu X and Ren Z (2019) Perilipin 5 protects against cellular oxidative stress by enhancing mitochondrial function in HepG2 cells. Cells 8, 1241
16. Yokota S, Nakamura K, Ando M et al (2014) Acetylcholinesterase (AChE) inhibition aggravates fasting-induced triglyceride accumulation in the mouse liver. FEBS Open Bio 4, 905-914
17. Li Y, Chao X, Yang L et al (2018) Impaired fasting-induced adaptive lipid droplet biogenesis in liver-specific Atg5-deficient mouse liver is mediated by persistent nuclear factor-like 2 activation. Am J Pathol 188, 1833-1846
18. Geisler CE, Hepler C, Higgins MR and Renquist BJ (2016) Hepatic adaptations to maintain metabolic homeostasis in response to fasting and refeeding in mice. Nutr Metab (Lond) 13, 62
19. Asimakopoulou A, Engel KM, Gassler N et al (2020) Deletion of perilipin 5 protects

against hepatic injury in nonalcoholic fatty liver disease via missing inflammasome activation. Cells 9, 1346

20. Gallardo-Montejano VI, Saxena G, Kusminski CM et al (2016) Nuclear Perilipin 5 integrates lipid droplet lipolysis with PGC-1alpha/SIRT1-dependent transcriptional regulation of mitochondrial function. Nat Commun 7, 12723

21. Nocetti D, Espinosa A, Pino-De la Fuente F et al (2020) Lipid droplets are both highly oxidized and Plin2-covered in hepatocytes of diet-induced obese mice. Appl Physiol Nutr Metab 45, 1368-1376

22. Du J, Hou J, Feng J et al (2019) Plin5/p-Plin5 guards diabetic CMECs by regulating FFAs metabolism bidirectionally. Oxid Med Cell Longev 2019, 8690746

23. Weber M, Mera P, Casas J et al (2020) Liver CPT1A gene therapy reduces diet-induced hepatic steatosis in mice and highlights potential lipid biomarkers for human NAFLD. FASEB J 9, 11816-11837

24. Lin X, Liu YB and Hu H (2017) Metabolic role of fibroblast growth factor 21 in liver, adipose and nervous system tissues. Biomed Rep 6, 495-502

25. Chong HK, Biesinger J, Seo YK, Xie X and Osborne TF (2012) Genome-wide analysis of hepatic LRH-1 reveals a promoter binding preference and suggests a role in regulating genes of lipid metabolism in concert with FXR. BMC Genomics 13, 51

26. Oosterveer MH, Mataki C, Yamamoto H et al (2012) LRH-1-dependent glucose sensing determines intermediary metabolism in liver. J Clin Invest 122, 2817-2826

27. Wang C, Zhao Y, Gao X et al (2015) Perilipin 5 improves hepatic lipotoxicity by inhibiting lipolysis. Hepatology 61, 870-882

28. Khalil A, Cevik SE, Hung S, Kolla S, Roy MA and Suvorov A (2018) Developmental Exposure to 2,2',4,4'-Tetrabromodiphenyl Ether Permanently Alters Blood-Liver

Balance of Lipids in Male Mice. Front Endocrinol (Lausanne) 9, 548

29. Seitz C, Huang J, Geiselhoringer AL et al (2019) The orphan nuclear receptor LRH-1/NR5a2 critically regulates T cell functions. Sci Adv 5, eaav9732

30. Lee JM, Lee YK, Mamrosh JL et al (2011) A nuclear-receptor-dependent phosphatidylcholine pathway with antidiabetic effects. Nature 474, 506-510

31. Mason RR and Watt MJ (2015) Unraveling the roles of PLIN5: linking cell biology to physiology. Trends Endocrinol Metab 26, 144-152

32. Harris LA, Skinner JR, Shew TM, Pietka TA, Abumrad NA and Wolins NE (2015) Perilipin 5-Driven Lipid Droplet Accumulation in Skeletal Muscle Stimulates the Expression of Fibroblast Growth Factor 21. Diabetes 64, 2757-2768

Fig. 1.

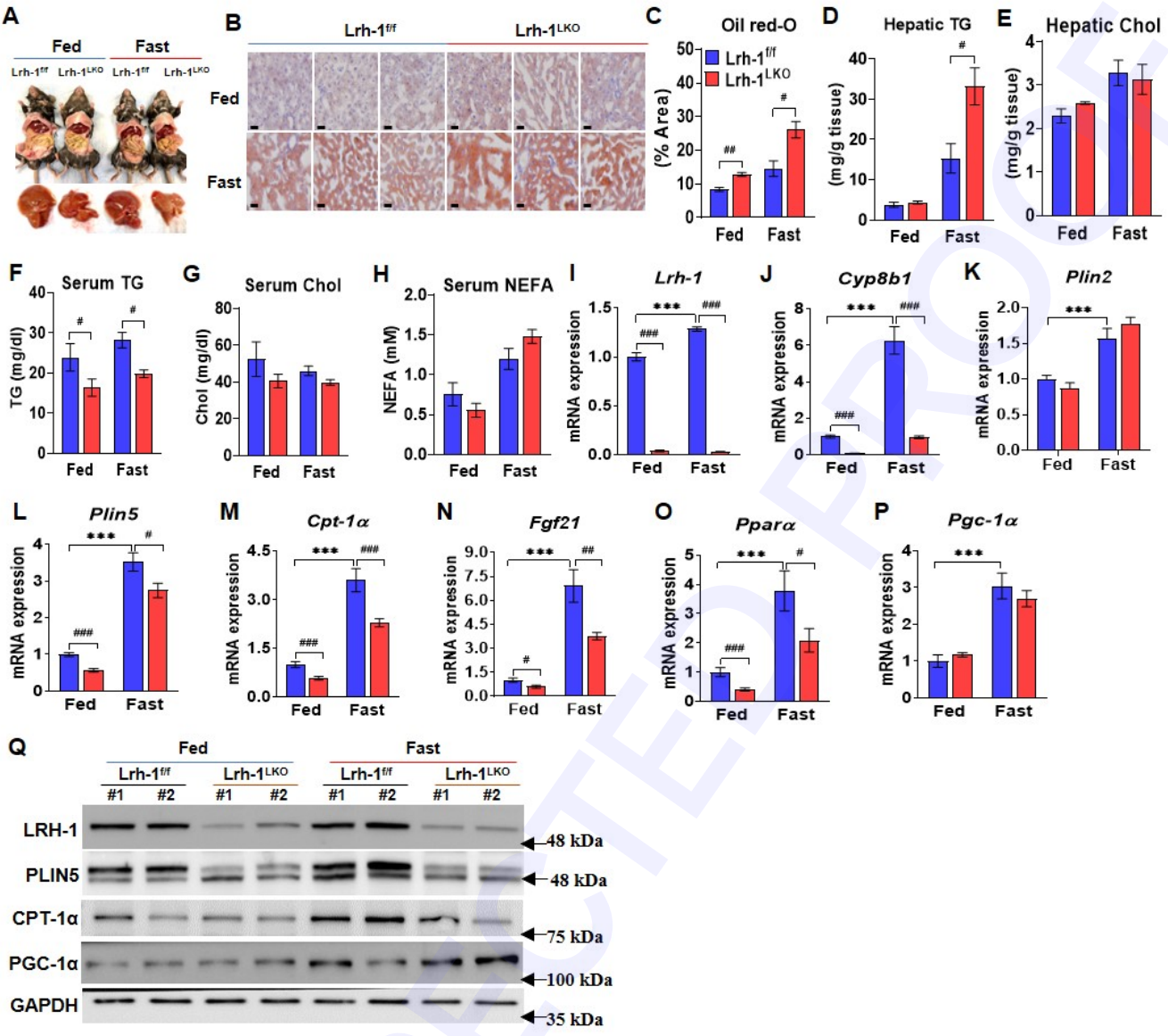

Fig. 1.

Fig. 2.

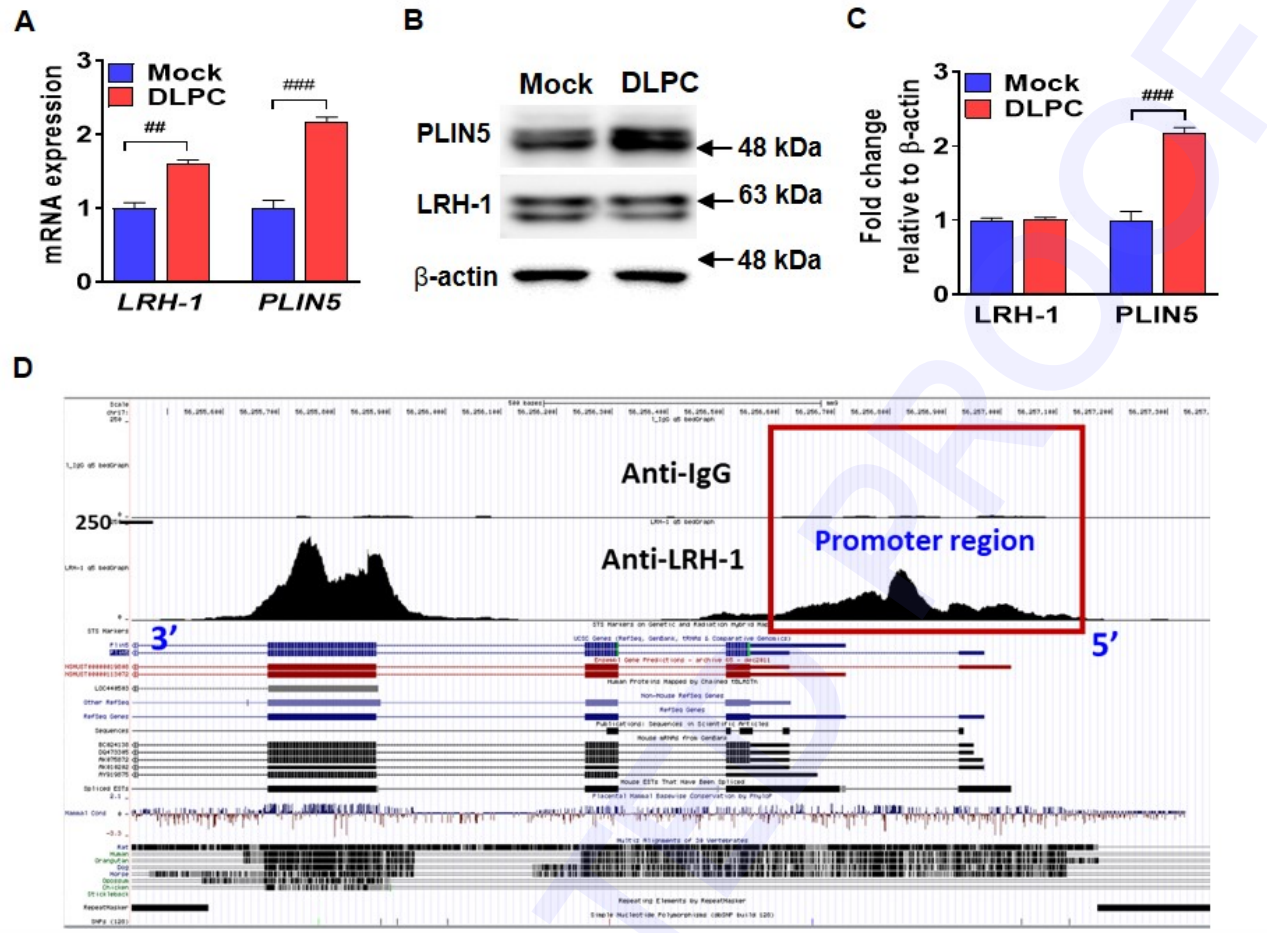

Fig. 2.

Fig. 3.

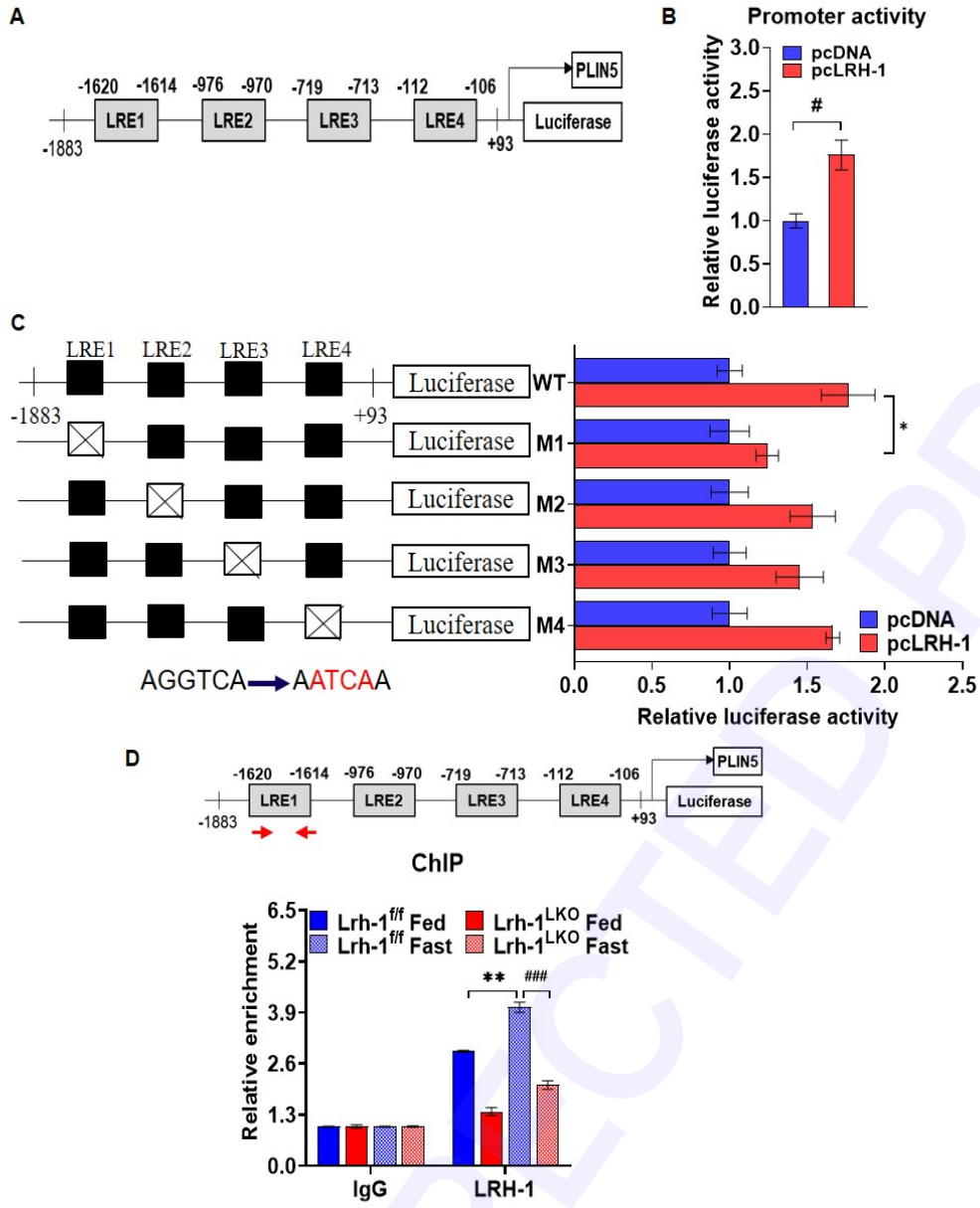

Fig. 3.

Fig. 4.

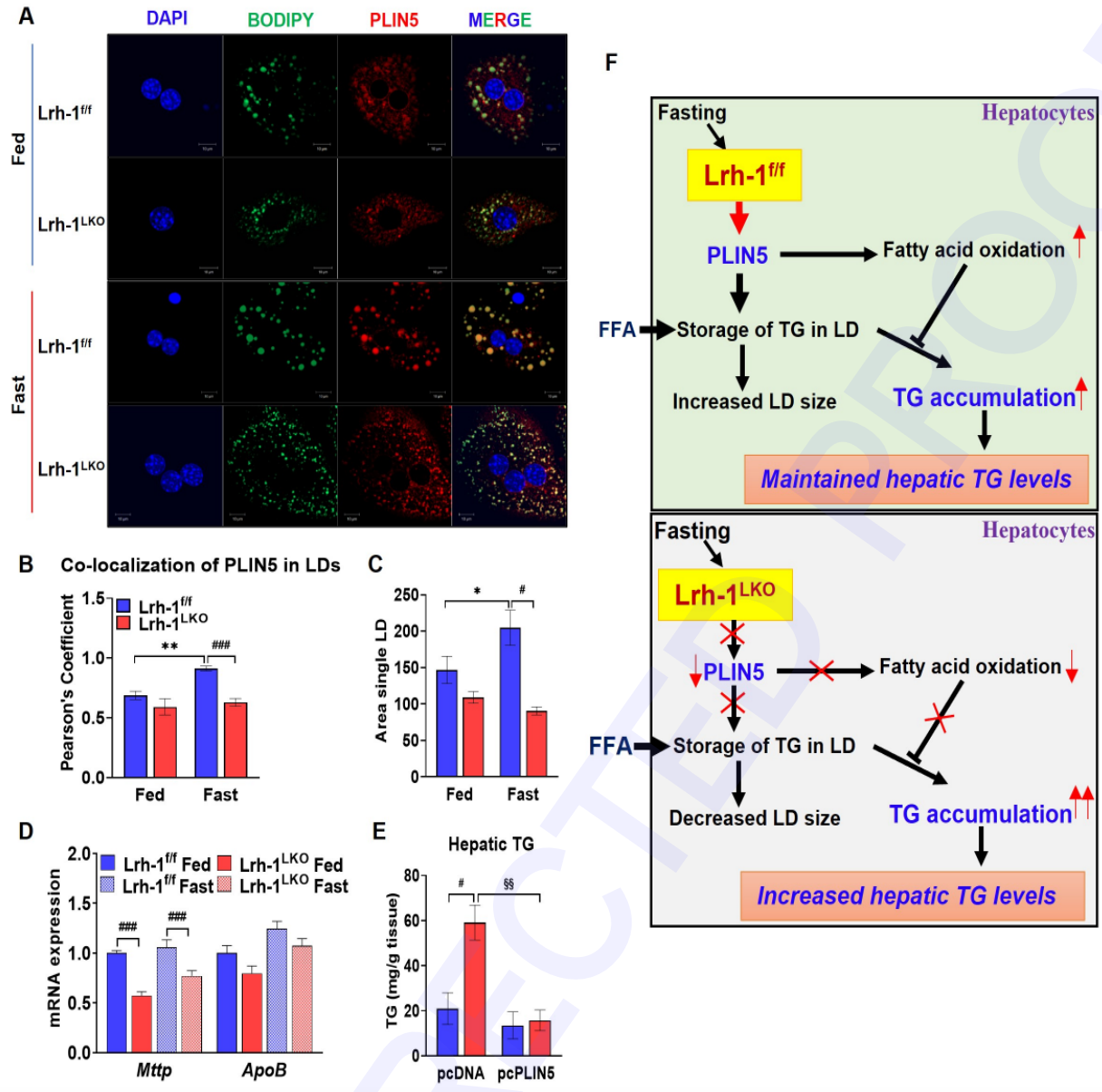

Fig. 4.

Supplementary materials

Perilipin 5 is a novel target of nuclear receptor LRH -1 to regulate hepatic triglycerides metabolism

Rubee Pantha[1], Jae-Ho Lee[1], Jae-Hoon Bae[1], Eun Hee Koh[2], Minsang Shin[3], Dae-Kyu Song[1], Seung-Soon Im[1*]

MATERIALS AND METHODS

Animal studies

Lrh-1$^{f/f}$ and Lrh-1^{LKO} mice were obtained by mating an LRH-1 allele flanked by LoxP sites (LRH-1$^{f/f}$) mice with albumin-Cre transgenic mice. LRH-1$^{f/f}$ mice were Kindly gifted by Prof. Timothy F. Osborne and albumin-Cre transgenic mice were purchased from The Jackson Laboratory (Bar Harbor, Maine, USA). Eight-to-twelve-week-old Lrh-1$^{f/f}$ and Lrh-1^{LKO} male mice were used. Mice were housed in a specific pathogen-free facility and fed a standard chow diet and water *ad libitum*. All mice were kept under 12:12-h light-dark cycles (6 a.m.-6 p.m. light, 6 p.m.-6 a.m. dark) at 22-24°C and 60-70% humidity. All animal experiments were performed following the guidelines provided by the Institutional Animal Care and Use Committee of Keimyung University (KM-2020-12R1).

Cell culture

HepG2 immortalized human hepatocytes and human embryonic kidney (HEK)-293T cells were cultured in Dulbecco's modified Eagle's medium (DMEM, Hyclone, Logan, UT, USA) supplemented with 10% fetal bovine serum (FBS, Hyclone) and 100 U/ml penicillin-streptomycin (P/S) as complete media. For LRH-1 agonist treatment, HepG2 cells were cultured in the presence or absence of 100 μM dialauroylphosphatidylcholine (DLPC, Sigma-Aldrich, Co., St. Louis, MO, USA) in DMEM complete media for 24 h. Primary hepatocytes were cultured in either William's Medium E (Gibco, Grand Island, NY, USA) supplemented with 10% FBS, 1% Glutamax (Gibco), and 100 U/ml P/S or DMEM media (Hyclone) supplemented with 10% FBS and 100 U/ml P/S. Cells were incubated in a humidified atmosphere containing 5% CO_2 at 37°C.

Quantitative polymerase chain reaction (qPCR)

Total RNA was isolated from the liver samples of 24 h-fasted and fed Lrh-1$^{f/f}$ and Lrh-1^{LKO} mice, as well as from HepG2 cells treated with the LRH-1 agonist DLPC, using TriZol reagent (Life Technologies, Carlsbad, CA, USA). The qPCR was performed using a CFX96^{TM} real time system (Bio-Rad, Hercules, CA, USA) to measure the expression level of various genes. Primer sequences used are listed in Supplementary Table 1. The relative mRNA expression level was normalized to ribosomal protein L32 or ribosomal phosphoprotein P0 by calculations based on the delta-delta threshold cycle method.

Western blot analysis

Western blot analysis was performed as described previously (1). Briefly, protein samples were collected from the liver tissues of 24 h-fasted and fed Lrh-1$^{f/f}$ and Lrh-1^{LKO} mice, as well as from LRH-1 agonist-treated HepG2 cells. Anti-LRH-1 from Aviva System Biology (San Diego, CA 92111 USA), anti-PLIN5 from Invitrogen (Carlsbad, California, USA), anti-CPT-1α from Santa Cruz Biotechnology (Dallas, Texas, USA), anti-PGC-1α from Abcam (Cambridge, MA, USA), anti-β-actin from Sigma Aldrich (Steinheim, Germany), and anti-GAPDH from Cell Signaling Technology (Danvers, MA, USA) antibodies were purchased. Antibody dilution and catalog number is listed in Supplementary Table 2. Horseradish peroxidase-conjugated mouse and rabbit secondary antibodies were used for the detection of protein bands. Antigen–antibody binding was detected using a chemiluminescent detection reagent (Bio-Rad).

Plasmid DNA design and transient transfection

The promoter region of mouse *PLIN5* from −1883 to +93 was synthesized by PCR, and the band size was confirmed by running it on an agarose gel. Then, the band was extracted by gel

extraction and cloned into the pGL3 basic vector, which was designated as pmPLIN5-1883/+93. In the promoter region, putative LRH-1-binding sequences were marked and deleted by site-directed mutagenesis using a Quick-change II Site-Directed Mutagenesis kit (Agilent Technologies Inc., Santa Clara, CA, USA). For transfection, HEK-293T cells were seeded on 6-well plates, and cells were transfected with pmPLIN5 with or without a murine LRH-1 and pCMV-β-galactosidase expression vector. The next day, 100 μM DLPC was administered to the cells, which were incubated for 24 h. Finally, cells were lysed in reporter lysis buffer (Promega corporation, Madison, WI 53711 USA) and luciferase assays were performed. The luciferase activity was normalized by β-galactosidase activity (2). For siPLIN5 overexpression, HepG2 cells were transfected with SMARTpool ON-TARGETplus Human PLIN5 siRNA (L-033568-01-0020, Dharmacon Inc., Colorado, USA). And as a control (D-001810-10-05, Dharmacon) were used. Next day, DLPC was treated to the cells and incubated for 24 h and total RNA was isolated.

Lipid analysis

For lipid extraction, livers were homogenized in 2:1 (v/v) chloroform:methanol three times followed by drying under a stream of nitrogen gas. These dried samples were resuspended in 1:1 (v/v) chloroform:methanol and 50 mM lithium chloride (LiCl) solution, and the lower layer was collected after centrifugation at 1400 × g for 10 min. To the upper layer, chloroform was added, and the sample was re-centrifuged to collect the lower layer, which was repeated twice. Samples that were collected three times were pooled together and dried in a stream of nitrogen gas. Subsequently, dried samples were processed again and resuspended in 1:1 (v/v) chloroform:methanol maintaining the concentration of LiCl at 10 mM. After centrifugation, the lower layer was collected, and the aforementioned procedure was consecutively followed

to collect the dried samples. To the dried sample, chloroform was added, and the sample was vortexed. Finally, TG and cholesterol were quantified with the TG-S and ASAN SET total-cholesterol kits (Asan pharm. Co., Gyeonggi-do, Korea) respectively, according to the manufacturer's instructions. Lipid contents were normalized to the liver tissue weight. Similarly, serum TG and cholesterol were analyzed using the TG-S and ASAN SET total-cholesterol kit. Serum NEFA levels were determined utilizing the NEFA C kit (Wako, Osaka, Japan).

Isolation and culture of primary hepatocytes

Hepatocytes were isolated from the livers of Lrh-$1^{f/f}$ and Lrh-1^{LKO} mice fed or fasted for 24 h using the perfusion method as described previously (3). Briefly, mice were anesthetized with isoflurane (Hana Pharm. Co., Gyeonggi-Do, Korea) and laparotomy was performed to uncover the portal vein. Then, the vein was catheterized and the liver was perfused with Earle's balanced salt solution (EBSS; WELGENE Inc., Gyeongsan, Republic of Korea) and 0.5 M ethylene glycol-bis(β-aminoethyl ether)-N,N,N′,N′-tetraacetic acid (EGTA), which was followed by 40 μg/ml liberase perfusion (Roche Diagnostics, Indianapolis, IN, USA) containing EBSS and 2 M $CaCl_2 \cdot H_2O$. Next, the liver was instantly detached and gently minced with 1× EBSS and 2 M $CaCl_2 \cdot H_2O$. Then, cells were filtered through a 100-μm nylon cell strainer followed by centrifugation of the filtrate at 50 × *g* for 1 min at 4°C. Subsequently, the pellet was re-suspended in Percoll buffer (GE Healthcare, Uppsala, Sweden) and re-centrifuged at 100 × *g* for 10 min at 4°C to collect the pellet. Finally, the cell pellet was gently resuspended in William's Medium E (Gibco) supplemented with 10% FBS, 1% Glutamax, and 100 U/ml P/S, successively plating the cells on collagen-coated culture dishes for 3~4 h.

LD staining

To mark LDs with Oil red-O, Lrh-$1^{f/f}$ and Lrh-1^{LKO} mice were sacrificed after feeding or fasting for 24 h and livers were removed immediately. The liver samples were cut into 10-µm sections and fixed with 4% paraformaldehyde for 10 min at room temperature. Similarly, for staining lipid droplets via BODIPY (Invitrogen), primary hepatocytes isolated from Lrh-$1^{f/f}$ and Lrh-1^{LKO} mice were seeded on an 8-well chamber. Cells were grown overnight either in fed (DMEM, 10% FBS, 1% P/S) or in fasting (DMEM, 2% lipoprotein deficient serum, 1% P/S) media. The next day, hepatocytes were fixed with 4% paraformaldehyde for 10 min at room temperature. Then, cells were treated with blocking solution (1% bovine serum albumin in dulbecco's phosphate-buffered saline) for 30 min followed by overnight incubation with a PLIN5 antibody (NB110-60509, Novus Biologicals, Centennial, CO, USA) at 4°C. The next day, cells were treated with a secondary antibody (Alexa Fluor 594, Invitrogen) and incubated for 1 h in the dark at room temperature. Subsequently, cells were stained with 2 µM BODIPY™ 493/503 (D3922; Invitrogen) and incubated for 10 min at room temperature. Finally, cells were covered with mounting medium and then observed using confocal laser scanning microscopy (Carl Zeiss, Thornwood, NY, USA).

ChIP assay

ChIP assay was performed as described previously (4). Briefly, chromatin was prepared from liver tissue of Lrh-$1^{f/f}$ and Lrh-1^{LKO} mice fed or fasted for 24 h. Liver tissues were minced and crosslinked with 1% paraformaldehyde and rotated for 8 min at room temperature. Crosslinking was stopped by adding 0.125 M glycine, and then, samples were rotated for an additional 5 min at room temperature. Finally, total chromatin was extracted from liver tissues and sonicated enough to obtain DNA fragments of 200–500 bp. Next, DNA were subjected to ChIP

using an anti-LRH-1 antibody (sc-393369X) from Santa Cruz Biotechnology (USA), and then qPCR was performed.

Liver-specific PLIN5 overexpression mice model

For overexpression of PLIN5, Lrh-$1^{f/f}$ and Lrh-1^{LKO} mice were injected in tail vein with 200 µl of PLIN5 overexpression or pcDNA vector using *in vivo*-JetPEI®-Gal (202-10G, Polyplus-transfection Inc., New York, NY, USA) transfection agent according to the instructions provided by the manufacturer. All mice were injected with pcDNA or PLIN5 overexpression or vector for two days. In the subsequent day, all mice were fasted for 24 h and then livers were isolated to measure TGs levels.

Electrophoretic mobility shift assay

To prepare the LRH-1 enriched nuclear extract protein, Hek293T cells were transfected with LRH-1 overexpression vector for 2 days. Cells were pelleted by centrifugation at 1000 × g for 5 min at 4 °C for and resuspended with buffer A (10 mM HEPES/KOH pH 7.6, 1.5 mM MgCl2, 10 mM KCl, 5 mM ethylenediaminetetraacetic acid (EDTA), 5 mM EGTA, 250 mM sucrose) supplemented with protease inhibitors and incubated on ice for 15 min. By centrifuging at 1000 × g for 7 min at 4 °C, pellet was resuspended in buffer B (20 mM HEPES/KOH pH 7.6, 1.5 mM MgCl2, 0.42 M NaCl, 1 mM EDTA, 1 mM EGTA, 2.5% glycerol) supplemented with protease inhibitors. Finally, nuclear extract was separated via centrifugation at 55,000 rpm for 30 min at 4 °C.

The single stranded complementary oligonucleotides including -1620/-1614 region of the PLIN5 promoter sequence were annealed to obtain double stranded DNA fragments. These DNA fragments were labeled with 32P radioisotopes and incubated with LRH-1 overexpressed

nuclear extract protein. The DNA-nuclear extract protein complexes were resolved in 9% non-denaturing polyacrylamide gel. After electrophoresis, the gels were dried, and visualized DNA-LRH-1 complex by autoradiography. For competition experiment, unlabeled DNA fragments (Cold DNA x 50) were added to nuclear extract.

Serum ketone bodies

Serum was isolated from the blood samples of Lrh-1$^{f/f}$ and Lrh-1^{LKO} mice fed or fasted for 24 h. To measure serum ketone bodies, serum β-Hydroxybutyrate levels was analyzed using MAK041-1KT (Sigma-Aldrich) kit according to the manufacturer's instructions.

Statistical analysis

Data were analyzed utilizing GraphPad Prism 8.4 software (GraphPad Software Inc., San Diego, CA, USA). Data are presented as the mean ± SEM. Statistical differences between groups were analyzed using a two-tailed student's t-test. Differences with P-values < 0.05 were declared significant.

Supplementary Figure legends

Supplementary Fig 1. LRH-1 binds on mouse PLIN5 gene. (A) PLIN5 promoter sequence from -1 to -1883 from the transcriptional start site (+1). Arrows designates putative LRH-1 binding sites. (B) ChIP assay on putative LRE region of mouse PLIN5 exon was measured in Lrh-$1^{f/f}$ and Lrh-1^{LKO} livers. (n=3-4/group). $^{\#\#}p < 0.01$, Lrh-$1^{f/f}$ vs. Lrh-1^{LKO}.

Supplementary Fig 2. (A) Serum β-hydroxybutyrate levels in 24 h-fasted or fed Lrh-$1^{f/f}$ and Lrh-1^{LKO} mice. (B) mRNA expression of *Plin5* in PLIN5 overexpressed Lrh-$1^{f/f}$ and Lrh-1^{LKO} mice.

Supplementary Fig 3. LRH-1 binds between the -1620 and -1614 region on the PLIN5 promoter sequence. (A) Oligonucleotides including -1620/-1614 region of LRH-1 binding sites on PLIN5 promoter sequence. (B) Annealing of complementary oligonucleotides and resolved in 9% non-denaturing gel. (C) EMSA of DNA-LRH-1 overexpressed nuclear extract complex in 2-fold serial dilution. (D) Competitive EMSA with cold DNA x 50. EMSA, electrophoretic mobility shift assay.

Supplementary Fig 4. siRNA of PLIN5 was transfected in HepG2 cells. (A) mRNA expression of *PLIN5*. (B, C) mRNA expression of *PPARα* and *PGC-1α*. $^{***}p < 0.001$, $^{**}p < 0.01$, siCont Mock vs. siCont DLPC, $^{\#\#}p < 0.01$, $^{\#}p < 0.05$, siCont Mock vs. siPLIN5 DLPC.

Supplementary Table legend

Supplementary Table 1. List of primers and their sequence used in qPCR. *ApoB*, apolipoprotein B; *Cpt-1α*, carnitine palmitoyltransferase 1 alpha; *Cyp8b1*, cytochrome p450 8b1; *Fgf21*, fibroblast growth factor 21; *Lrh-1*, liver receptor homolog-1; *L32*, ribosomal protein L32; *Mttp*, microsomal triglyceride transfer protein; *Pgc-1α*, peroxisome proliferator-activated receptor gamma coactivator 1-alpha; *Plin2*, perilipin 2; *Plin5*, perilipin 5; *Pparα*, peroxisome proliferator-activated receptor alpha; *RPLP0*, ribosomal protein lateral stalk subunit P0.

Supplementary Table 2. List of primary antibodies used in western blotting.

Supplementary Fig 1.

A

-1883	CCCACCCTCTGCCTTATGTTTTAAGACAGGATCTCTGGCCGGGCGGTGGTGGCGCATGCCTTTGATCCCAGCACTTGGGAGGCAGA	-1798
-1797	GGCAGGTGGATTTCTGAGTTCGAGGCCAGCCTGGTCTACAGAGTGAGTTGCAGGACAGCCAGGGCTACACAGAGAAACCCTGTCT	-1713
-1712	CGGGAAAATAAATAAATAAAAAATCTCTGACTGGCCAGCTGAGAGCCTCGGGATCTTTCTGCCTCTTTCTCTGCCTCTGCCTCCCAG	-1626
-1625	AGCTGAGGTCACACACATGAGCCAGTGTCACACATGACAAATGTGTCAAATTGAGGTCTTCCGGCTTACATGATAAGTGATAAGCA	-1540
-1539	CTTTACTGACAGTGACTGCTCTCCAGATCCTTCCCACTGTATAGCCCTGACTCTCCTGGAACTTGCTCTGTAAGCTGGCTGGTCTCAA	-1452
-1451	AGTCAGAGGTCCTCCTGCCTCTACCTCCTGAGTGCTGGGATTAAAGTCCTGCATCACAACCCAGCTTTAGTTTTTTTCACCCCCTAG	-1365
-1364	ACAGAGGGACTCTGCCCATTGAGAGGCAGGGGTGTGGATTTTTTTTTTAAAGGCCCGGTTTCATATTGCCCAGGCTGGCCTCAAATT	-1278
-1277	TGCTATAAGCCTAGGGTGATTTGAGCTCATGATTCTCCTGTCTCCACCTTGTGGCTCTGGGTGACAAGCATATGACTGGGCAAAACT	-1191
-1190	AGGCTTCTCACCCCAGTCCTGCAGAGGGAGCTGGGGAGAGTGGGTTAAAACTTGGGTCTCAGTTTGCTGATCTGTAAAATGGGGTC	-1105
-1104	AGAACTGACAGGCTTAACAGCTCTCAGGATTAAACAGCAGATTAAAAATAAGATGGAGGCCAGAGAGACCACCCATGGCTTAACA	-1020
-1019	GCTCAGGCTGGAGTTCCAGTCCCAGCATCCACATGATAGCTCAAGGTCACATGTTACTCCAGTCACAGGGGGTCTGTCAACTTTACT	-933
-932	GGCCTCTGTGGGGATCAGGCATCTGTGGATCATGACAGATGGAACATATCAACAAAACACCAGGACACATAGACGTAATAATAAT	-848
-847	AATAACAAAGGAAGTGGGCCTCAGAAGGCAGTCAGCCGAGCACCCACAGATCTGGGTTCACGCCCAGCACCACATAAACATGTGT	-763
-762	GGTGTGGCACATCTGTTGTCTTAGCCACTGGGTGGTGCGTTCAAGGTCATCCTTGGCTATGTGGTTACTTTGAGGCTATCCTGGGCT	-676
-675	ATATAGTGAGTTCTGGTCAAGTCTTGACTACAGAGAGAGAGTCTGAATCAAACAAAACAAACGGAAAAGACTGAAGAATGAGAA	-592
-591	AGTCGCCGGGCGTGGTGGCTCATGCCTTTAATCCCAGCACTTGGGAGGCAGAGGCAAGGTGGATTTCTGAGTTCGAGGCCAACCTG	-506
-505	ATCTACAAAATGAGTTCCAGGATAGCCAGAGAAAACCTGTCACAAAAAACAAAACAAAACAAAACAAAAAAAAAACAACAAAAG	-422
-421	AAGAAGGAGGAGGAGGAGGAGAAAAAAGGAGGAGGAGAAAAAAGAGGAGAAGGAGAAGGAGAAGGAGAAGGAGAA	-341
-340	GGAGAAGGAGAAAGAAGAAGAAAAGTCCTCAGTCGCCGGGCGGATTTCTGAGTTCGAGGCCAGCCTGTTCGGTCTACAGAGTGAG	-256
-255	TTCCAGGACAGCCAGAGCGATACAGAGAAACCCTGTCTCGAAAAAACCAACCAACCAACCAACCAAAAACCAACCAACCAACCA	-172
-171	ACCAACCAATCAAACAAACAAACAACAACAACAAAAAGAAAGTCCTCAGTCCTAGTCTGAGGTCAGCCATGGTGACTGGACCAGG	-87
-86	ATTCAGCGTCCCTGAGCCGCTATGGCAACCATGGCGCCTGTGGGGGGCGGGGAAGCTCCAGATCCACCCCCGGCGGCGCCTCATTG	-1

B

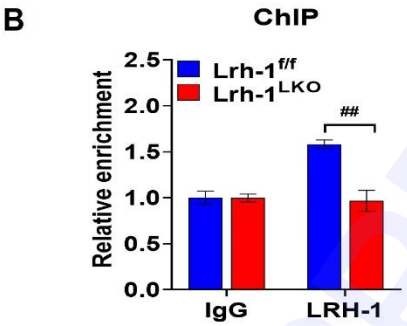

Supplementary Fig 2.

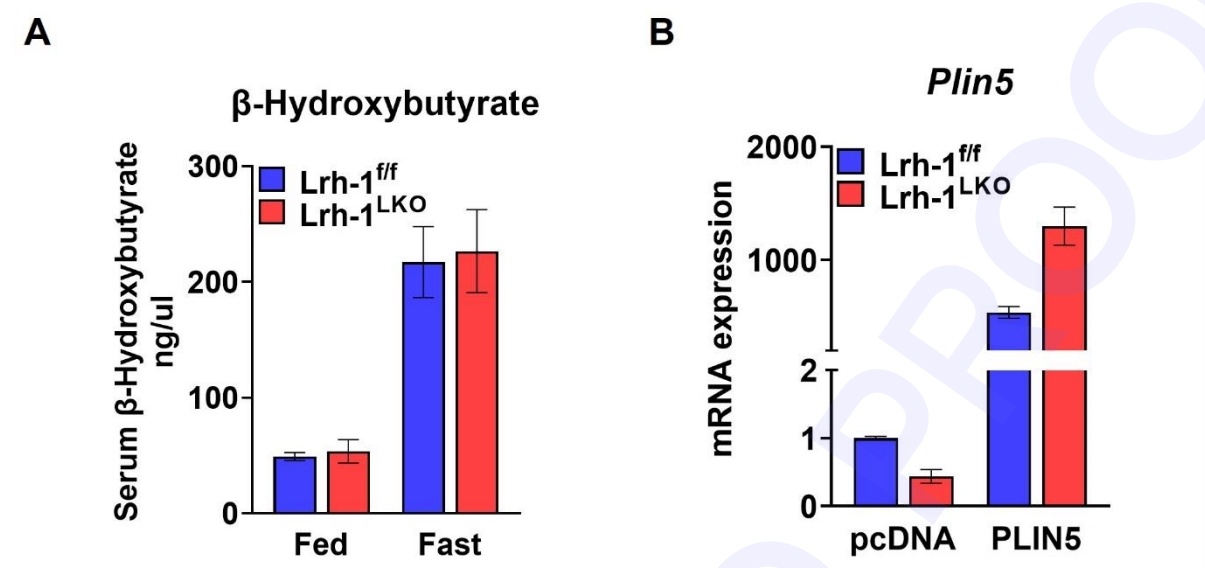

Supplementary Fig 3.

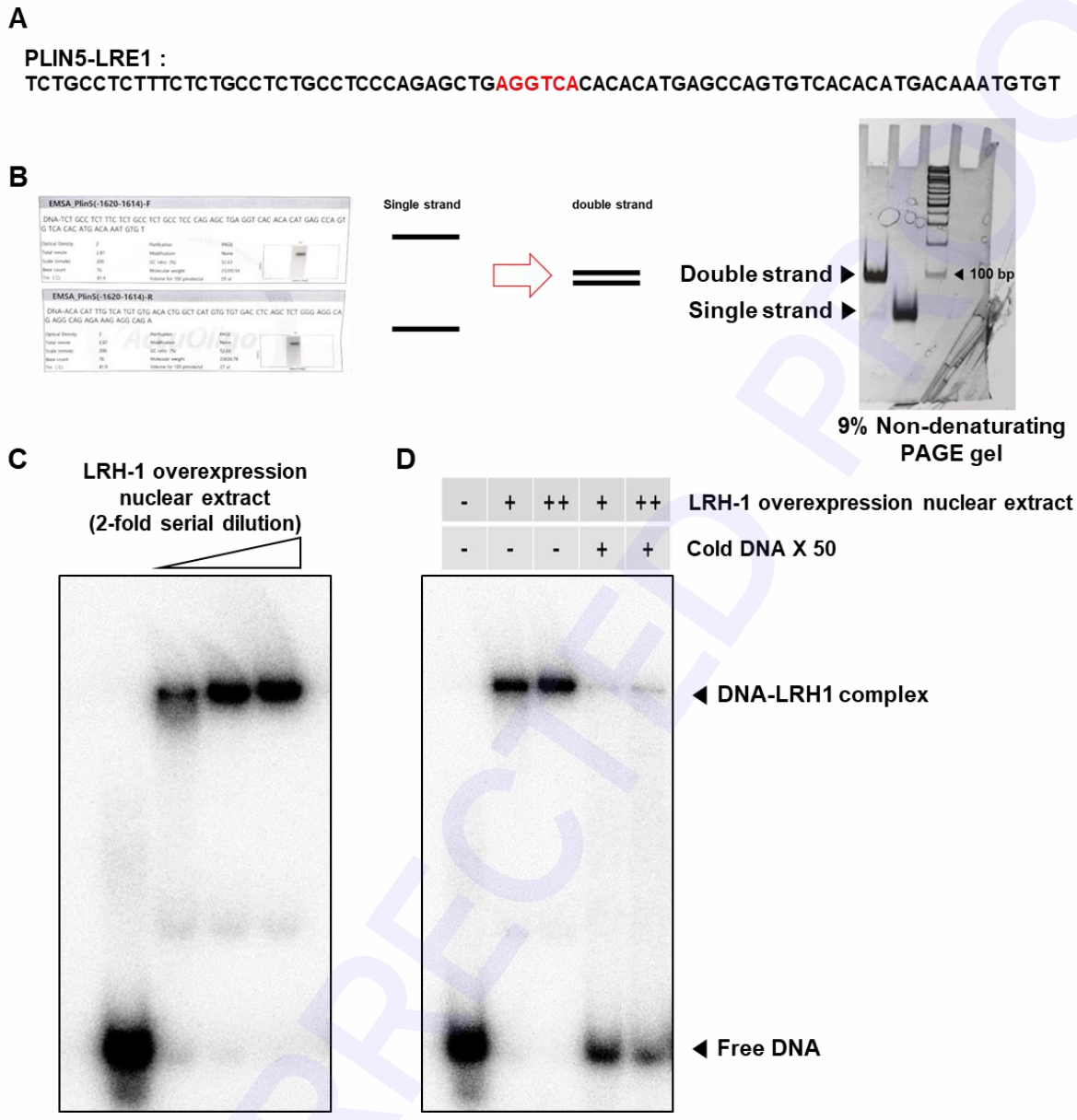

Supplementary Fig 4.

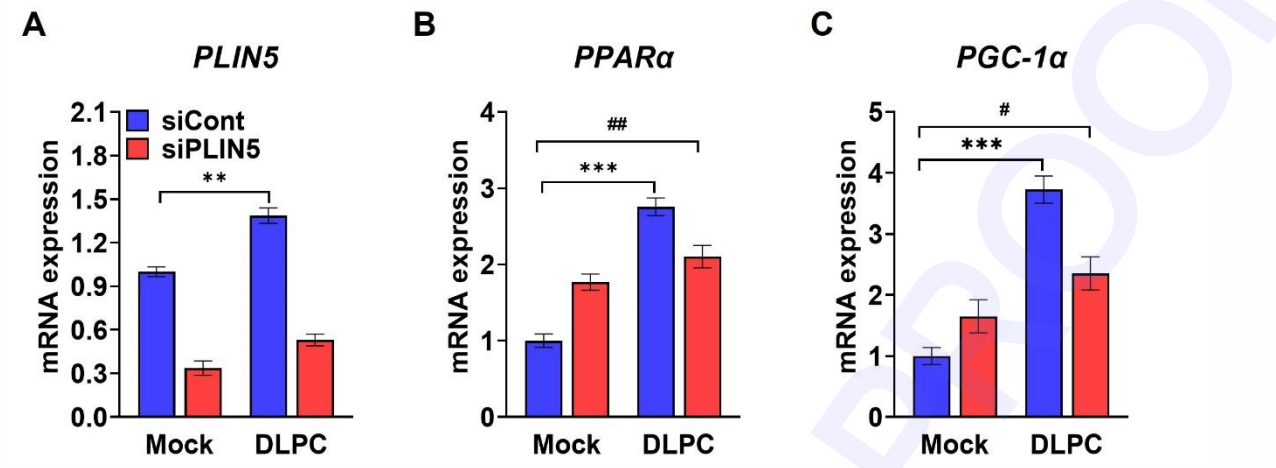

Supplementary Table 1. List of primers and their sequence used in qPCR.

Gene	Species	Forward primers (5'→3')	Reverse primers (5'→3')
L32	Mouse	ACATTTGCCCTGAATGTGGT	ATCCTCTTGCCCTGATCCTT
Lrh-1	Mouse	TCATGCTGCCCAAAGTGGAGA	TGGTTTTGGACAGTTCGCTT
Plin5	Mouse	TGTCCAGTGCTTACAACTCGG	CAGGGCACAGGTAGTCACAC
Plin2	Mouse	CCTCAGCTCTCCTGTTAGGC	CACTACTGCTGCTGCCATTT
Cyp8b1	Mouse	CAAAGCCCCAGCGCCT	TTCGACTTCAAGCTGGTCGA
Cpt1-α	Mouse	CTCCGCCTGAGCCATGAAG	CACCAGTGATGATGCCATTCT
Fgf21	Mouse	CTGCTGGGGGTCTACCAAG	CTGCGCCTACCACTGTTCC
Pparα	Mouse	AGAGCCCCATCTGTCCTCTC	ACTGGTAGTCTGCAAAACCAAA
Pgc-1α	Mouse	CAAACCCTGCCATTGTTAAG	TGACAAATGCTCTTCGCTTT
Mttp	Mouse	CTCTTGGCAGTGCTTTTTCTCT	GAGCTTGTATAGCCGCTCATT
ApoB	Mouse	TTGGCAAACTGCATAGCATCC	TCAAATTGGGACTCTCCTTTAGC
RPLP0	Human	GTGCTGATGGGCAAGAAC	AGGTCCTCCTTGGTGAAC
LRH-1	Human	CTTTGTCCCGTGTGTGGAGAT	GTCGGCCCTTACAGCTTCTA
PLIN5	Human	AGGCTGACGCAGAAGAATTG	AACAGAAGGCATTGGGCAAA
PPARα	Human	TTCGCAATCCATCGGCGAG	CCACAGGATAAGTCACCGAGG
PGC-1α	Human	TGAAGACGGATTGCCCTCATT	GCTGGTGCCAGTAAGAGCTT

Supplementary Table 2. List of primary antibodies used in western blotting.

Primary antibody	Catalog number	Dilution
LRH-1	ARP37407_P050	1:1000
PLIN5	PA1-46215	1:1000
CPT-1α	sc-393070	1:1000
PGC-1α	ab54481	1:1000
GAPDH	2118	1:1000
β-actin	A5441	1:1000

References

1. Lee JH, Go Y, Kim DY et al (2020) Isocitrate dehydrogenase 2 protects mice from high-fat diet-induced metabolic stress by limiting oxidative damage to the mitochondria from brown adipose tissue. Exp Mol Med 52, 238-252
2. Lee JS, Bae S, Kang HS, Im SS and Moon YA (2017) Liver receptor homolog-1 regulates mouse superoxide dismutase 2. Biochem Biophys Res Commun 489, 299-304
3. Im SS, Kang SY, Kim SY et al (2005) Glucose-stimulated upregulation of GLUT2 gene is mediated by sterol response element-binding protein-1c in the hepatocytes. Diabetes 54, 1684-1691
4. Im SS, Hammond LE, Yousef L et al (2009) Sterol regulatory element binding protein 1a regulates hepatic fatty acid partitioning by activating acetyl coenzyme A carboxylase 2. Mol Cell Biol 29, 4864-4872